Flow through Curved Rectangular Channels of Large Aspect Ratio

Matthew J. Targett, William B. Retallick, and Stuart W. Churchill
Dept. of Chemical Engineering, University of Pennsylvania, Philadelphia, PA 19104

Numerical solutions were obtained for the field of velocity in angular forced flow through the annulus between two concentric cylinders of large and infinite aspect ratio with a gap-to-inner radius ratio of 0.05 using a finite-element representation and the FIDAP code. For an infinite aspect ratio, velocity vectors reveal a purely angular motion below a critical Dean number of 37.31 and a secondary motion in the form of pairs of counterrotating vortices above that value. The wavelength of these vortices and the friction factor are correlated in terms of the Dean number. For large but finite aspect ratios a weak secondary motion around the periphery is found to occur below the critical Dean number, while for greater values the vortex at each end of the channel is greatly extended. The computed patterns of flow are in good agreement with prior experimental visualizations as well as with those carried out as part of this investigation. The computed characteristics are also in good agreement with prior theoretical results for limiting cases. The adaptation of the results for flow through an Archimedean spiral is described.

Introduction

The overall objective of the investigation, of which the work reported here is a small but essential element, is to characterize theoretically and experimentally the thermal and chemical behavior of a combined heat exchanger/catalytic reactor in the form of a compact double spiral. As indicated by Retallick et al. (1990) and Targett et al. (1992), such a device has promise for the destruction of contaminants, including aerosols and microorganisms, in air from confined living and working spaces.

The use of a double-spiral heat exchanger has also been proposed for other applications that require the minimization of heat losses and/or volume, including the combustion of low-heating-value gases that cannot be burned without significant preheating (see, for example, Jones et al., 1978).

Vertical and cross-sectional views of a double-spiral heat exchanger with inflow and outflow of the same stream and with an electrical heat input at the core are sketched in Figure 1. The stream of air, which enters one of the spiral passages at the periphery, is heated by exchange with the same stream of air flowing outward from the plenum through the other spiral passage. An incremental quantity of heat is supplied to the air by an electrical resistance element in the plenum. The relative angular locations of the entrances and exits of the two spiral passages are arbitrary but do influence the thermal behavior somewhat, especially for a small number of turns (Targett et al., 1991; Choudhury et al., 1985).

A particular advantage of the double-spiral configuration is to minimize heat losses by exposing only the outer turn and the ends to the surroundings. (In a conventional countercurrent heat exchanger the total length of at least one passage is exposed to the surroundings.) Minimal heat losses are critical to the performance of a double-spiral heat exchanger in both of the applications just mentioned in that the energy supplied to the plenum by combustion or an electrical heater must be small relative to that which is exchanged.

In the air cleaner, both sides of the corrugated metal sheets of which the exchanger is constructed are coated with a thin layer of catalyst. The catalyst is of course omitted from the portions of the surface facing the surroundings and the plenum. The process of catalytic oxidation of the contami-

Correspondence concerning this article should be addressed to S. W. Churchill.
Current addresses of: M. T. Targett: E. I. duPont Co., Wilmington, DE 19880; W. B. Retallick: W. B. Retallick Associates, 1432 Johnny's Way, West Chester, PA 19382.

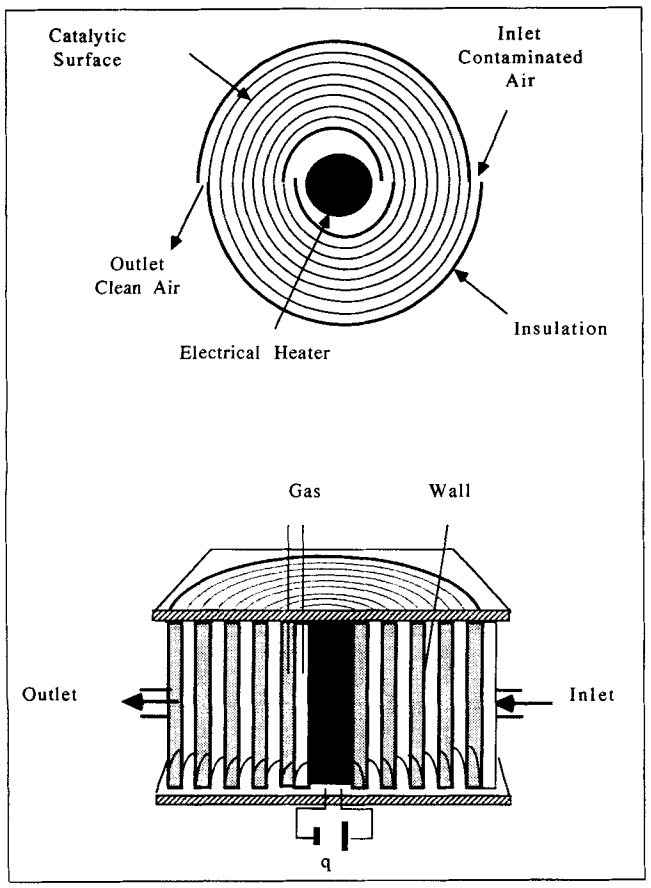

Figure 1. Four-turn spiral.

nants is dependent on a sufficient fraction of the coated surface attaining a high enough temperature. Although the process of destruction of the contaminants involves mass transfer to the surface and reaction on the surface as well as heat transfer, it can be characterized satisfactorily for a given geometry and rate of flow by a single representative temperature such as that of the air leaving the plenum. The prediction of the attainment of such a characteristic temperature requires complete thermal modeling of the exchanger, including heat losses to the surroundings and internal thermal radiation. The process of convective heat exchange in a double spiral is quite complicated even in a purely geometrical sense in that the entering stream receives heat from the exiting stream through the inner wall of the channel and also, depending on the location and the conditions, receives heat from or loses heat to the exiting stream one turn later through the outer wall of the channel (see Figure 1). Targett et al. (1991) have developed analytical solutions in closed form for exchangers with a limited number of spiral turns. These solutions reveal semiquantitatively the unique behavior of double-spiral exchangers, but incorporate one sweeping idealization, namely the invariance throughout the exchanger of the product of the local heat-transfer coefficient and the associated area. The area for heat exchange per unit angle decreases toward the plenum while, because of the intensifying secondary motion associated with the decreasing radius of curvature, the local heat-transfer coefficient increases but not necessarily to the same degree. The local heat-transfer coefficient also depends strongly on the ratio of the local heat flux densities on the opposing walls.

In order to predict the local coefficient of heat transfer in a spiral passage it is necessary to know the detailed velocity field, including the secondary motion, at each point in the exchanger. The objective of the work reported here has been to develop a numerical solution for the field of flow in spiral passages for a range of conditions corresponding to those to be encountered in the proposed air cleaner, and also to confirm the validity of these numerical solutions with experimental visualizations.

In the interests of generality the numerical solutions reported herein are for isothermal and isobaric conditions. The temperature is actually expected to vary considerably and the pressure to vary measurably over the exchanger in the applications of interest. On the other hand, the variations of the temperature and pressure across the narrow dimension of a channel are expected to be small at all locations within the exchanger. Hence the isothermal and isobaric results presented herein are expected to be applicable locally to a good approximation in thermal calculations. The fluid motion, as modeled, is postulated to be time-independent and nonturbulent—restrictions that provide an upper limit to the physical validity of the solutions with respect to the rate of flow as characterized by the Reynolds number or the Dean number.

The results presented in this article are limited to the fluid motion. Results for the associated thermal behavior, which is dependent on additional physical properties and additional imposed conditions, will be presented separately.

Prior Work

No results, either theoretical or experimental, appear to have been published for flow through a spiral channel with a rectangular cross section. The only theoretical work for flow in a spiral of any kind appears to be that of Baurmeister and Brauer (1979). They constructed a solution for an Archimedean spiral of circular cross section by approximating the velocity field at a series of distances through the spiral with that for fully developed flow in a torus with the corresponding radius of curvature. The elemental solutions for toroidal flow that were used in this procedure were obtained by finite-difference calculations.

Forced flow in a complete torus due to a pressure gradient, such as that modeled by Baurmeister and Brauer, is in itself purely hypothetical. This idealization has, however, also been widely used with some success to approximate flow through helical coils of small pitch. A few of these numerical solutions are for channels of rectangular cross section and thereby are directly relevant to the work reported herein. Flow through a torus with a rectangular cross section can also be conceived as angular flow in the annulus between two concentric circular cylinders.

The first work on angular flow in the annulus between concentric cylinders is apparently that by Dean (1928), who performed a linear stability analysis for cylinders of infinite length with an asymptotically small gap-to-inner-radius ratio d/r_1. His analysis is analogous to the well-known one of Taylor (1923) for the same geometry but with the inner cylinder rotating and the outer one fixed. Dean concluded from his

analysis that purely angular flow with fixed surfaces is stable for values of $Re_d(d/r_1)^{1/2}$ less than 35.94, but that a secondary motion in the form of pairs of counterrotating vortices with a wavelength-to-gap ratio $\alpha = \lambda/d$ of approximately $2/(1.57)^{1/2} = 1.60$ is stable for values of $Re_d(d/r_1)^{1/2}$ slightly greater than 35.94. This prediction of a critical value of $Re_d(d/r_1)^{1/2}$ for the onset of a secondary motion in angular flow between concentric cylinders is in contrast with the behavior in a coil of circular cross section, for which vortices are known to form for even incipient rates of flow. The dimensionless grouping $Re_d(d/r_1)^{1/2}$ or some slight perturbation thereof is now universally called the Dean number and symbolized by Dn.

Reid (1958) and others have used more refined methods to obtain the values $Dn_c = 35.92$ and $\alpha_c = 1.595$ for angular flow in a cylindrical gap of infinite aspect ratio with $d/r_1 \to 0$. Walowit et al. (1964) utilized the Galerkin method to determine the effect of a complete range of r_1/r_2 from 1 to 0.1 on the critical Dean number and wavelength. Using a four-term approximation, they computed $Dn_c = 35.90$ and $\lambda_c/d = 1.587$ for $r_1/r_2 \to 1$. For $r_1/r_2 = 0.95$, which corresponds closely to the condition of the current work, they computed $Dn_c = 37.20$ and $\lambda_c/d = 1.563$. Finlay et al. (1988) used a pseudospectral simulation similar to those developed for turbulent flows to determine $Dn_c = 36.592$ and $\alpha_c = 1.586$ for a finite inner-radius-to-gap ratio $r_1/d = 39$. They also predicted the onset of wavy steady-state vortices at $Dn \cong 50$ and the onset of undulating time-dependent flow at $Dn \cong 65$. Lingrani et al. (1992) have since carried out further simulations for the regimes of undulating and twisting vortices.

Brewster et al. (1959) were apparently the first to determine the critical Dean number and wavelength experimentally. Using both bubbles and a dye as a marker, they pumped aqueous solutions of glycerine through a sector of an annulus with an aspect ratio of 35 and an inner-radius-to-gap ratio of 12. The annulus was completely blocked at one angle. The circulating fluid entered through the inner wall near one side of the partition and exited near the other. They determined a critical Dean number of 36.5 ± 1.1 and a critical wavelength-to-gap ratio of 1.31 ± 0.25. The predicted values of the Dean number for the transitions to steady-state wavy flow and to time-dependent flow have been confirmed semiquantitatively by experiments. (See, for example, Ligrani and Niver, 1988; Lingrani et al., 1992.)

Although a number of numerical solutions have been carried out for flow in torii of square cross section (angular flow in a cylindrical gap of unitary aspect ratio), those for large but finite aspect ratios are very limited, presumably because of the extensive computational demands. Cheng and Akiyama (1970) utilized a finite-difference formulation with the postulate of an asymptotically small value of d/r_1 to compute the velocity field for aspect ratios of 2 and 5 (as well as for 1/5, 1/2, and 1). Cheng et al. (1976) subsequently carried out similar calculations for an aspect ratio of 2 (as well as for 1/5, 1/2, and 1) for finite radius-to-gap ratios. For $h/d = 2$, they chose $r_1/d = 132.8$ and 39.5. Their results include friction factors for a series of Dean numbers from 10.5 to 182 as well as velocity distributions and stream functions for representative conditions in that range.

Winters and Brindley (1984) utilized a finite-element formulation for the primary purpose of predicting the points of bifurcation for aspect ratios of 1 and 4 with $r_{ave}/d = 25$, but they also predicted streamlines and axial velocity contours for particular conditions. Winters (1987) subsequently presented similar results for aspect ratios of 1 and 2.

Finlay et al. (1988) determined the angular pressure gradient as a function of Re/Re_c from their computed velocity profiles, as well as the previously mentioned points of transition.

Several visual studies of the velocity field in addition to that of Brewster et al. (1959) have been carried out in half turns of rectangular cross section with a large aspect ratio. Kelleher et al. (1980) utilized an aspect ratio of 40 and $r_1/d = 46.6$. Their photographs of an aerosol mist indicate wavelength-to-gap ratios of about 1.6 for Dn of 69.3 and 77.2. Ligrani and Niver (1988) utilized the same aspect ratio and wavelength-to-gap ratio as Kelleher et al., but used mesquite-wood smoke for visualization. They did not observe complete vortices at their measuring station of $\theta = 115(2\pi/180)$ rad until Dn attained a value of 73, perhaps because of incomplete development of the flow. Their measured velocity distributions at $Dn = 36$ and $\theta = 120(2\pi/180)$ rad are in good agreement over the central portion of the gap with the theoretical expression presented below for subcritical flow in an annulus of infinite aspect ratio. Lingrani et al. (1992) carried out further measurements in the same equipment for the regimes of undulating and twisting flow and present contours of the time-mean velocity as well as power spectra.

None of the studies mentioned earlier provide the detailed information on the flow field that is required to predict heat-transfer coefficients for curved rectangular channels of large finite aspect ratio. The work described below has the objective of filling that void.

Asymptotic Solutions

A solution in closed form can readily be derived for the velocity distribution in subcritical angular flow due to a pressure gradient in the annulus between two concentric cylinders of infinite axial extent. The result (see, for example, Goldstein, 1938) for this hypothetical flow can be expressed as

$$u_\theta = \frac{r}{4\mu}\left(\frac{dP}{d\theta}\right)\left[\frac{1-(r_2/r)^2}{1-(r_2/r_1)^2}\ln\left\{\left(\frac{r_2}{r_1}\right)^2\right\} - \ln\left\{\left(\frac{r_2}{r}\right)^2\right\}\right]. \quad (1)$$

Integration of Eq. 1 over the annulus yields the following expression for the mean velocity:

$$u_{\theta m} = \frac{r_1^2}{8\mu(r_2 - r_1)}\left(-\frac{dP}{d\theta}\right) \times \left[\left(\frac{r_2}{r_1}\right)^2 - 1 - \frac{\left(\frac{r_2}{r_1}\right)^2\left(\ln\{(r_2/r_1)^2\}\right)^2}{(r_2/r_1)^2 - 1}\right]. \quad (2)$$

Equation 2 can also be expressed as

$$f_{ave}Re_d = \frac{16\left(\frac{r_2}{r_1}-1\right)^4}{\left[\left(\frac{r_2}{r_1}\right)^2-1\right]^2-\left(\frac{r_2}{r_1}\right)^2\left[\ln\left\{\left(\frac{r_2}{r_1}\right)^2\right\}\right]^2} \quad (3)$$

where

$$f_{ave} \equiv \frac{2(\tau_w r_1+\tau_{w2}r_2)}{(r_1+r_2)\rho u_{\theta m}^2} = \frac{d}{r_{ave}\rho u_{\theta m}^2}\left(-\frac{dP}{d\theta}\right). \quad (4)$$

Equation 3 can be expanded for small $d/r_1=(r_2/r_1)-1$ to obtain

$$f_{ave}Re = \frac{12}{1-\frac{1}{30}\left(\frac{d}{r_1}\right)^2-\ldots}. \quad (5)$$

Equation 5 indicates that subcritical flow in an annulus of infinite extent and small gap-to-radius ratio results in a slightly higher friction factor than flow between parallel plates, for which $fRe_d=12$. Equations 3 and 5 both predict that in subcritical flow, $f_{ave}Re_d$ is a function of d/r_1 (or r_2/r_1) but not of Dn.

Solutions in closed form have not been attained for angular subcritical flow in an annulus of finite aspect ratio, but the small effect of curvature indicated by the denominator of Eq. 4 suggests that the solution for fully developed laminar flow in a straight rectangular channel should be a lower bound and a good approximation for slightly curved flow. This solution, which was first derived by de Saint Venant (1855) in another context, can be expressed in terms of the coordinates of the annulus as

$$u_\theta = \frac{d^2}{8\mu r}\left(-\frac{dP}{d\theta}\right)\left[1-\left(1-\frac{2(r-r_1)}{d}\right)^2 + \frac{32}{\pi^3}\sum_{n=0}^{\infty}\frac{(-1)^{n+1}}{(2n+1)^3}\frac{\cosh\left\{(2n+1)\frac{\pi z}{d}\right\}}{\cosh\left\{(2n+1)\frac{\pi h}{2d}\right\}} \times\cos\left\{\frac{(2n+1)\pi}{2}\left(1-\frac{2(r-r_1)}{d}\right)\right\}\right]. \quad (6)$$

Integration of u_θ, as given by Eq. 6, over the half cross section $r_1 \le r \le r_2$, $0 \le z \le h/2$ gives

$$u_{\theta m} = \frac{d^2}{12\mu}\left(\frac{2}{r_1+r_2}\right)\left(-\frac{dP}{d\theta}\right)\psi\left\{\frac{h}{d}\right\} \quad (7)$$

where

$$\psi\left\{\frac{h}{d}\right\} = 1-\frac{192}{\pi^5}\left(\frac{d}{h}\right)\sum_{n=0}^{\infty}\frac{\tanh\left\{(2n+1)\frac{\pi h}{2d}\right\}}{(2n+1)^5}. \quad (8)$$

Equation 7 can be reexpressed in terms of the friction factor as

$$fRe_d = \frac{12}{\left(1+\frac{d}{h}\right)\psi\left\{\frac{d}{h}\right\}}. \quad (9)$$

For large aspect ratios the summation of Eq. 8 approaches 1.004524, hence

$$fRe_d \to \frac{12}{\left(1+\frac{d}{h}\right)\left[1-\frac{192}{\pi^5}(1.004524)\frac{d}{h}\right]} = \frac{12}{\left(1+\frac{d}{h}\right)\left(1-0.63025\frac{d}{h}\right)}. \quad (10)$$

Numerical Modeling

An axial segment of the channel to be modeled is shown in Figure 2 in order to define the variables. For a channel of infinite extent the distance b represents a trial value for the unknown wavelength λ of a pair of counterrotating vortices. For a channel of finite aspect ratio the distance b corresponds to $h/2$, the half-breadth of the channel.

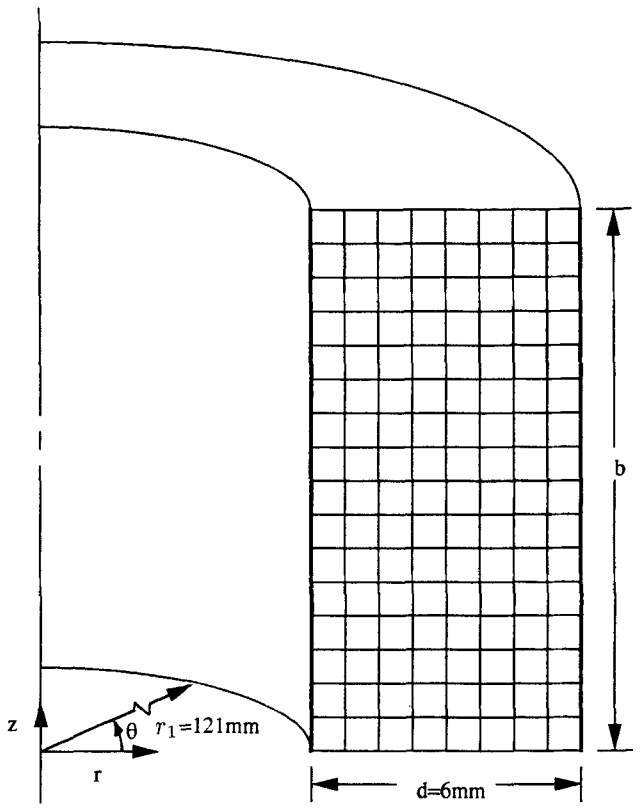

Figure 2. Grid arrangement for finite-difference computations.

The actual channel of interest consists of an Archimedean spiral (with a constant change of radius with angle), but in the numerical modeling the effect of the changing radius is neglected, that is, at each distance through the coil the velocity field is postulated to be the same as in fully developed angular flow in the annulus between two concentric cylinders. This is the same idealization as that made by Baurmeister and Brauer (1979) for a spiral coil of circular cross section, and is analogous to the idealization made by a number of investigators in neglecting the pitch of a helical coil.

The following additional postulates are made in the interests of simplicity:

1. invariant physical properties
2. Newtonian behavior
3. steady, axisymmetric, nonoscillatory flow

The postulate of axisymmetry eliminates all derivatives in θ except for the pressure, but all three balances for momentum and all three components of the velocity must be retained to allow for a secondary motion. The equation for the conservation of mass can then be written in polar cylindrical coordinates as

$$\frac{1}{r}\frac{\partial}{\partial r}(ru_r)+\frac{\partial u_z}{\partial z}=0 \tag{11}$$

and the equations for the conservation of momentum as

$$\rho\left(u_r\frac{\partial u_r}{\partial r}-\frac{u_\theta^2}{r}+u_z\frac{\partial u_r}{\partial z}\right) = -\frac{\partial P}{\partial r}+\mu\left[\frac{1}{r}\frac{\partial}{\partial r}\left(r\frac{\partial u_r}{\partial r}\right)+\frac{\partial^2 u_r}{\partial z^2}-\frac{u_r}{r^2}\right] \tag{12}$$

$$\rho\left(u_r\frac{\partial u_\theta}{\partial r}+\frac{u_r u_\theta}{r}+u_z\frac{\partial u_\theta}{\partial z}\right)=-\frac{1}{r}\frac{\partial P}{\partial \theta} + \mu\left[\frac{1}{r}\frac{\partial}{\partial r}\left(r\frac{\partial u_\theta}{\partial r}\right)+\frac{\partial^2 u_\theta}{\partial z^2}-\frac{u_\theta}{r^2}\right] \tag{13}$$

and

$$\rho\left(u_r\frac{\partial u_z}{\partial r}+u_z\frac{\partial u_z}{\partial z}\right)=-\frac{\partial P}{\partial z}+\mu\left[\frac{1}{r}\frac{\partial}{\partial r}\left(r\frac{\partial u_z}{\partial r}\right)+\frac{\partial^2 u_z}{\partial z^2}\right]. \tag{14}$$

The FIDAP (Fluid Dynamics International, Inc.) finite-element code that was used to solve these equations would not (logically enough) accept an angular pressure gradient for fully developed toroidal flow. Hence the angular pressure gradient was replaced by an equivalent body force, that is, $-(\partial P/\partial\theta)$ in Eq. 13 was replaced by ρG. Solutions for different pressure gradients were thereby generated by choosing a series of values of ρ. The value of G, which is arbitrary in this scheme, was chosen to be 1×10^{-3} m^2/s^2. Calculations were carried out somewhat differently for infinite and finite aspect ratios. The computations were implemented at the Pittsburgh Supercomputing Center on a Cray Y-MP.

Infinite aspect ratio

The calculations for an infinite aspect ratio were for a single wavelength since the velocity field is postulated to be periodic in this respect. This distance is not known in advance, so calculations were carried out for a series of axial distances b, and the wavelength was determined as the value of $b=\lambda$ for which the mean velocity in the angular direction is a minimum.

The boundary conditions consisted of no slip at r_1 and r_2, and those for symmetry at $z=0$ and $z=b$. The inner radius r_1 was chosen to be 121 mm and the outer radius r_2 to be 127 mm, resulting in an inner-radius-to-gap ratio $r_1/d=121/6=20.17$. A dynamic viscosity equal to 1.9×10^{-5} Pa·s was utilized.

The computational scheme involved a 17×25 mesh (in the r and z directions, respectively) with 425 nodal points and 384 elements. The elements were four-noded, quadrilateral, and linear. The components of the velocity were approximated by bilinear interpolation functions and the pressure by a piecewise discontinuous approximation. The penalty-pressure method was used with $\nabla\cdot v=1\times10^{-7}P$. The strategy of solution consisted of ten successive substitutive iterations followed by up to 500 quasi-Newton iterations. The tolerances for velocity convergence and force convergence were both set at 0.001. This tolerance was sufficient for close agreement with theoretical values for the critical Dean number and wavelength and with Eqs. 1 and 2 for subcritical values of the Dean number.

Computational Results

The determination of the wavelength for three values of the Dean number is illustrated in Figure 3, in which the computed mean velocity is plotted vs. the postulated wavelength b for three specified densities. The values of $u_{\theta m}$ and λ at the minimum of the curves, as well as the corresponding values of λ/d, Dn, and $f_{ave}Re_d$ for all of the calculations are listed in Table 1.

From the values in Table 1, the critical Dean number, as computed, is seen to fall between 35.666 and 38.794. Linear

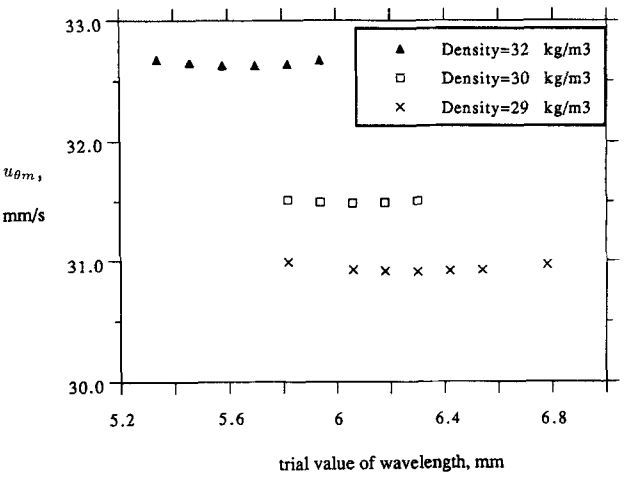

Figure 3. Determination of wavelength of vortices in a channel of infinite aspect ratio.

Table 1. Friction Factors and Wavelengths Determined Computationally for an Infinite Aspect Ratio

ρ	$u_{\theta m}$			$f_{ave}Re_d$		
kg/m^3	mm/s	Dn	λ/d	Comput.	Eq. 3	Eq. 15
5	6.341	2.230	—	12.05	12.0009	
10	12.68	8.917	—	12.05	12.0009	
15	19.02	20.06	—	12.05	12.0009	
20	25.36	35.67	—	12.05	12.0009	
21	26.27	38.79	1.67	12.21		12.33
22	26.85	41.54	1.53	12.52		12.66
23	27.40	44.32	1.46	12.83		12.93
24	28.00	47.26	1.39	13.10		13.19
25	28.60	50.28	1.31	13.36		13.44
26	29.17	53.33	1.21	13.62		13.67
27	29.74	56.47	1.15	13.87		13.89
28	30.32	59.70	1.09	14.11		14.11
29	30.91	63.03	1.05	14.36		14.33
30	31.49	66.43	1.01	14.56		14.54
34	33.76	80.72	0.90	15.39		15.36
40	36.96	103.96	0.725	16.54		16.52

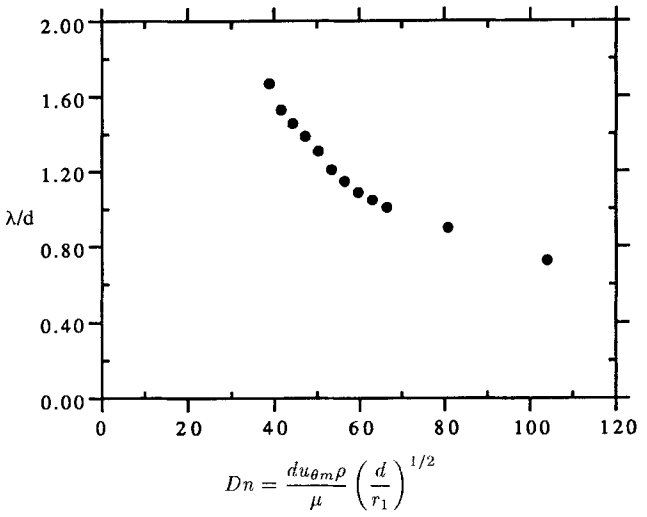

Figure 4. Computed wavelength for vortices in a channel of infinite aspect ratio.

extrapolation of the larger values of $f_{ave}Re_d$ to 12.056 yields $Dn_c = 37.31$, which is consistent with the theoretical value of 35.92 obtained from stability analysis for $d/r_1 \to 0$, the value of 37.20 determined by Walowit et al. (1964) for $r_1/d = 19$, and the value of 36.592 computed by Finlay et al. (1988) for $r_1/d = 39$. The corresponding value of $\lambda_c/d = 1.67$ is slightly above the theoretical values of ~ 1.6. In view of the insensitivity of the determination of λ, as illustrated in Figure 3, such a small discrepancy is not surprising.

The theoretical value of $f_{ave}Re$ for subcritical values of Dn is predicted by Eq. 3 to be 12.00094 for $r_2/r_1 = 127/121$. The slight but consistent discrepancy (0.4%) with the computed values in Table 1 for subcritical values of Dn is presumed to represent the net error of the computed values in this respect.

The computed wavelength ratios are plotted vs. Dn in Figure 4. These values are in good agreement with a curve of Finlay et al. (1988) (in their Figure 6) for the wavelength ratio corresponding to the maximum pressure gradient for a given value of Dn.

The computed velocity vectors corresponding to $Dn = 38.79$ and $Dn = 103.96$ are plotted in Figure 5. The intensity of the circulation may be noted to increase and the wavelength to decrease as Dn increases.

The computed values of $f_{ave}Re_d$ for supercritical values of Dn are seen in Table 1 to be represented within 1% by the following empirical expression based on the canonical form proposed by Churchill and Usagi (1972):

$$f_{ave}Re_d = 12.05\left[1+\left(\frac{Dn-37.31}{130}\right)^{3/4}\right]^{2/3} \qquad (15)$$

On the presumption that the combining exponent of 3/2 and the coefficient of 130 do not change, Eq. 15 can be generalized as

$$f_{ave}Re_d = (f_{ave}Re_d)_l\left[1+\left(\frac{Dn-Dn_c}{130}\right)^{3/4}\right]^{2/3} \qquad (16)$$

where $(f_{ave}Re_d)_l$ and Dn_c represent the appropriate values for any r_1/d as given by Eq. 3 and by Walowit et al. (1964), respectively.

The values of $f_{ave}Re_d$ and λ/d in Table 1 for supercritical values of Dn are based on the postulate of a series of steady symmetrical pairs of counterrotating vortices, and hence are presumed to be valid only up to values of Dn for which this mode of flow remains physically stable. The constraint applies to Eq. 15 and to the graphical correlation in Figure 4. The values of $f_{ave}Re_d$ and λ/d in Table 1 are for a single value of $r_1/d = 20.17$, but are implied to be a function of Dn only rather than separately of Re_d and r_1/d. The range of validity of this postulate is unknown.

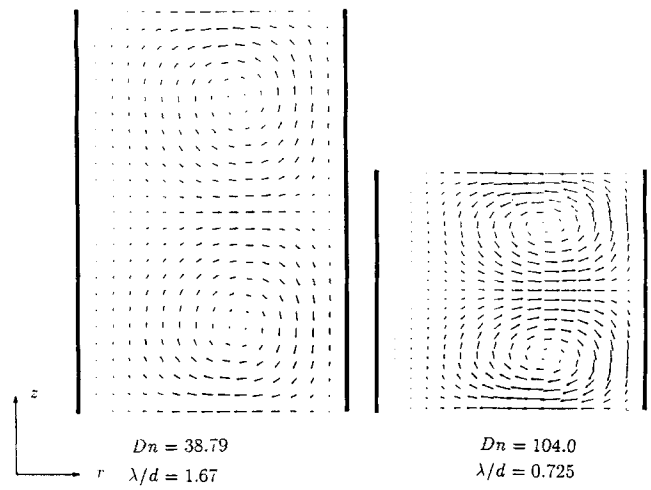

Figure 5. Computed velocity vectors for secondary motion in a channel of infinite aspect ratio (Dn_c = 37.31).

Table 2. Computed Friction Factors for Large Finite Aspect Ratios

	ρ kg/m^3	$u_{\theta m}$ mm/s	Dn	$f_{ave}Re_d$
$h/d = 5$				(11.442)*
	20	21.845	30.72	11.658
	21	22.553	33.30	11.857
	22	23.544	36.42	11.749
	23	24.444	39.53	11.981
	24	25.595	43.20	11.940
$h/d = 12$				(11.691)*
	19.0	22.664	30.28	11.824
	19.5	23.242	31.87	11.831
	19.7	23.480	32.53	11.834
	19.9	23.712	33.18	11.837
	20.0	23.829	33.51	11.838
	21.0	24.987	36.90	11.854
	21.5	25.564	38.65	11.862
	21.8	25.508	39.10	12.054
	22.0	25.665	39.70	12.091
$h/d = 16$				(11.757)*
	20.0	24.192	34.02	11.889
	21.0	25.377	37.47	11.901
	21.6	26.086	39.62	11.908
	21.8	25.804	39.56	12.150
	22.0	25.875	40.03	12.228

*From Eq. 9.

Finite aspect ratios

In order to determine the effect of the ends of the channel on the fluid motion in the annulus between two concentric cylinders of finite length, finite-element calculations were carried out for aspect ratios of 5, 12, and 16. The only significant difference in the modeling for these finite aspect ratios as compared to that described earlier for an infinite aspect ratio arises from the boundary conditions in the axial direction; the condition of symmetry at the unknown distance $z = b$ was replaced by the condition of no slip at $z = h/2$. Also, since the ratio $h/2d$ for each of the three of the specified aspect ratios was greater than λ/d for the infinite aspect ratio, a greater number of finite elements was necessary. In order to maintain approximately the same ratio of elements per vortex as for the infinite aspect ratio, grids of 17×45, 13×72, and 13×88 were used for aspect ratios of 5, 12, and 16, respectively.

The computed values of $f_{ave}Re_d$ for a series of Dean numbers encompassing the critical value are listed in Table 2. Values of $f_{ave}Re_d$ computed from Eq. 9 are included for reference.

Velocity vectors for values of Dn just below and just above that for the formation of vortices are plotted in Figures 6, 7, and 8. A secondary motion in the form of a boundary-layer-

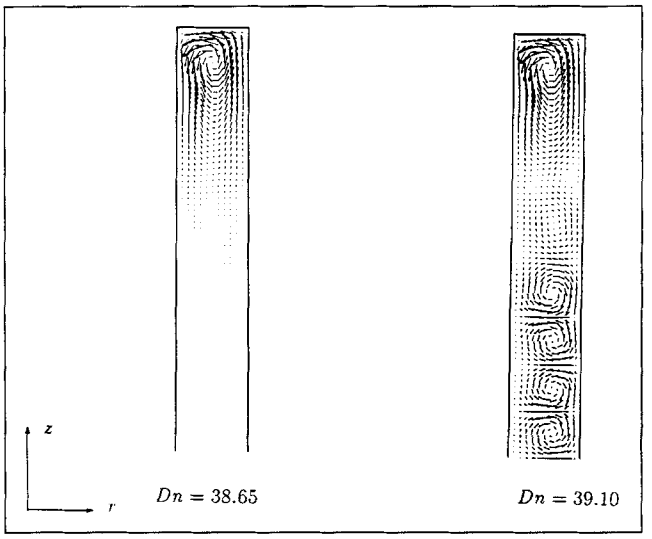

Figure 7. Computed velocity vectors for secondary motion in a channel with an aspect ratio of 12 ($Dn_c \cong 39$).

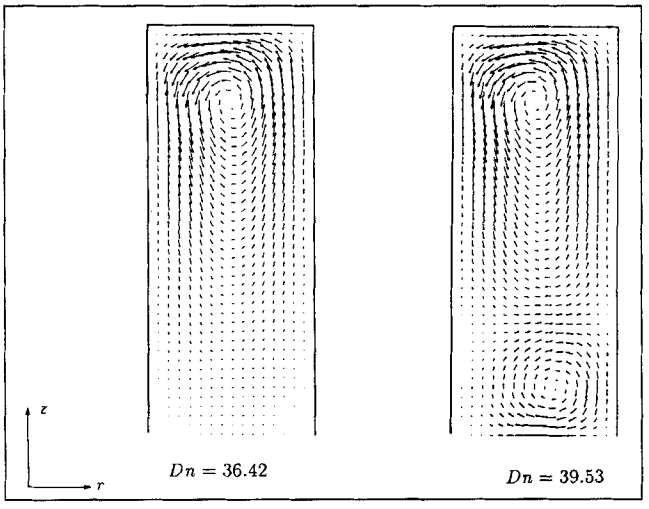

Figure 6. Computed velocity vectors for secondary motion in a channel with an aspect ratio of 5.0 ($Dn_c \cong 39$).

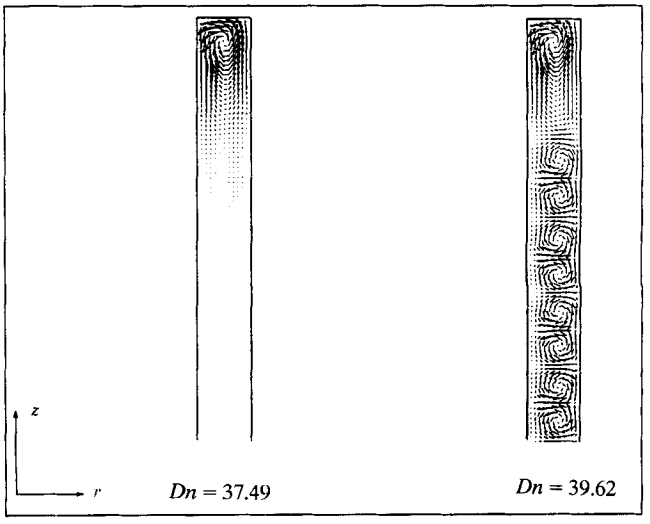

Figure 8. Computed velocity vectors for secondary motion in a channel with an aspect ratio of 16 ($Dn_c \cong 39$).

like flow around the entire periphery of the channel is apparent for the subcritical values of Dn.

This behavior is in contrast with that in an unbounded annulus for which no secondary motion occurs below the critical value of the Dean number. For subcritical flow the boundary-layer-like motion would be expected to result in a slightly higher Poiseuille number $Po = f_{ave}Re_d$ than for a straight channel of the same cross section, a slight increase in Po with the rate of flow (as represented by the Dean number) for the same aspect ratio, and an increase in the rate of flow (as represented by $u_{\theta m}$ and Dn) with an increase in the aspect ratio for a given body force (as represented by ρ). All three of these effects can be discerned from the values in Table 1. (The decrease in Po with decreasing aspect ratio for a given value of Dn is an artifact of basing f on the average shear stress on all four surfaces; $-dP/d\theta$ itself increases.)

The circulation for slightly supercritical values of the Dean number is seen in the half-region of Figures 5, 6, and 7 to consist of one or more pairs of equally sized vortices plus one pair with one much larger half-cell.

The computed velocity vectors for $h/d = 12$ are compared in Figure 9, with a photograph of the motion by Cheng et al. (1977) for essentially the same conditions. The agreement in form is very good.

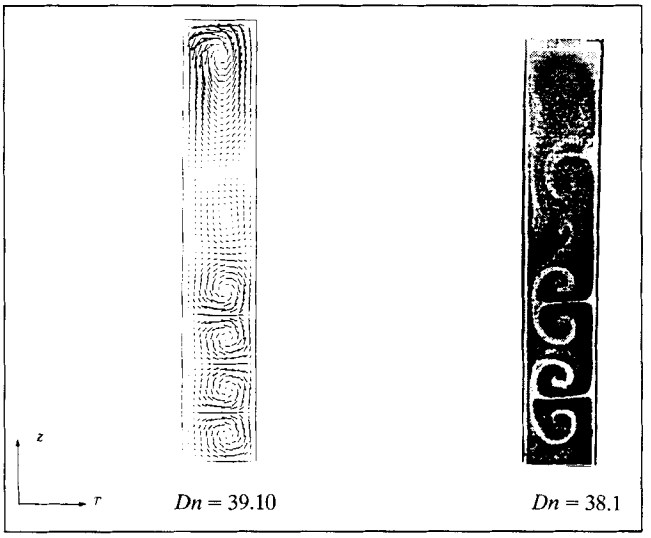

Figure 9. Comparison of computed velocity vectors for secondary motion in a channel of aspect ratio of 12 with a photograph of Cheng et al. (1977).

Visualization Study

The visualizations mentioned earlier by Brewster et al. (1959), Kelleher et al. (1980), and Ligrani and Niver (1988) all involved flow in a sector of a circular annulus. In order to provide a more realistic simulation of flow in a spiral, a visualization study was carried out in the apparatus shown in Figure 10. As indicated, this device was constructed in the form of six half-cylinders of discretely increasing radius. This geometry is a close approximation of an Archimedean spiral. The channel was actually formed from three sections of round Plexiglas tubing with radii of 202.3 mm, 228.6 mm, and 254 mm, each 292.1 mm in length and 3.175 mm in thickness. The three sections of tubing were cut once axially and forced into pseudo spiral grooves, 3.175 mm deep and slightly greater than 3.125 mm wide, in square endplates of Plexiglas, 304.8 mm on a side and 9.525 mm thick. The cylinders were fastened into the grooves and to one another with acrylic cement. This construction resulted in a channel with a width of 6.35 mm, a length of 295.75 mm, and an average radius of 111.2 mm. Hence $h/d = 46.6$ and $r_{ave}/d = 17.51$.

The experimental fluid was water and the visualization agent was 0.1 wt. %, finely ground mica and powdered titanium dioxide pigment (Mearlin). The tracer-laden water was circulated inwardly through the spiral with a pump. The rate of circulation was measured with a rotameter. The fluid in the inner turn was illuminated with a 150-W slide projector containing a slide with a 2-mm-wide slit. Photographs were taken in the direction normal to the plane of illumination with a 35-mm camera and a 90-mm telemacro lens. Kodak Gold ASA100 film was exposed for 0.25 s at an f-stop of 32. This technique of visualization is similar to that used by Cliffe and Mullin (1985) to observe Taylor vortices between rotating cylinders.

A black and white copy of a colored photograph of the motion is shown in Figure 11. The uniform gradations caused by the secondary motion are most evident in the innermost channel (on the right) because of the higher Dean number of 41 and the longer entrance length of 1.5 turns. Only one vortex of each counterrotating pair is visible in the photograph. The observed value of the wavelength was approximately 1.6 times the spacing between the walls. At elevated rates of flow corresponding to $Dn \geq 45$, a secondary circulation was no longer visible, and the occurrence or nonoccurrence of the transitions to steady-state wavy flow and to undulating time-dependent flow as predicted by Finlay et al. (1988) could not be observed.

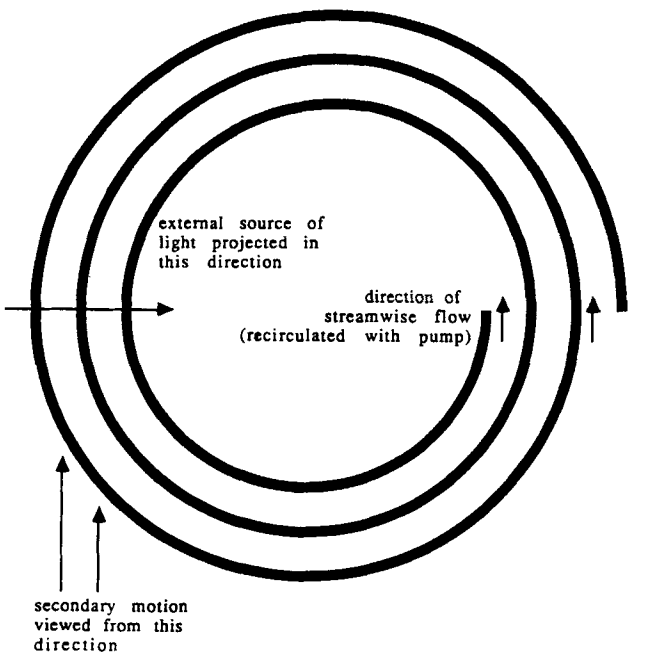

Figure 10. Apparatus for flow visualization.

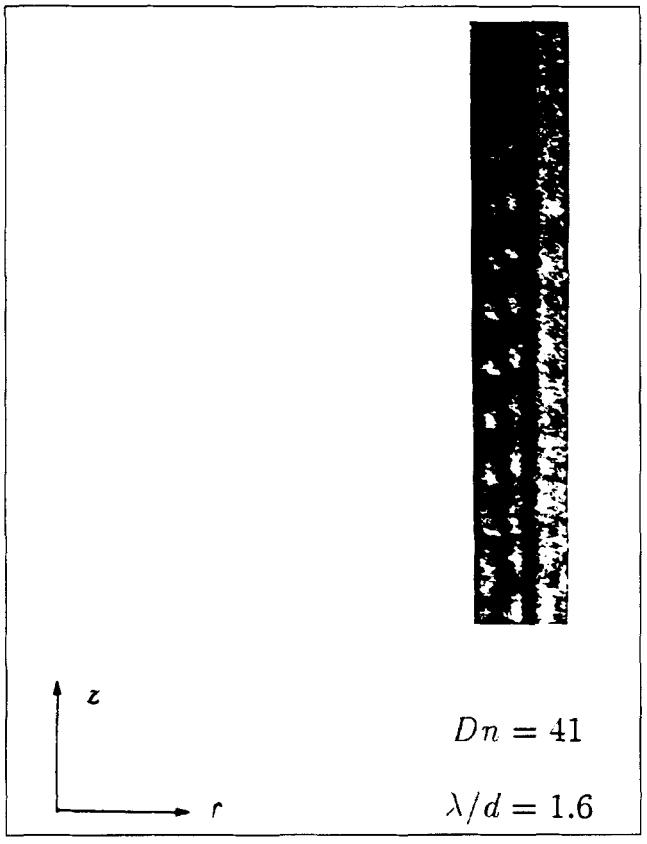

Figure 11. Observed secondary motion in a channel with an aspect ratio of 44.

Friction Factor for a True Spiral

The friction factor for fully developed angular flow in an annulus of infinite aspect ratio is predicted by Eq. 3 for $Dn \leq Dn_c$ and by Eq. 16 for $Dn \geq Dn_c$. These predictions are postulated to provide a good approximation for the local friction factor in an Archimedean spiral of infinite aspect ratio if Dn, Dn_c, and $(f_{ave}Re_d)_l$ are evaluated at the corresponding values of

$$\frac{r_1}{d} = \frac{r_0 \pm \beta x}{d}, \qquad \frac{r_{ave}}{d} = \frac{r_0 \pm \beta x}{d} + \frac{1}{2},$$

$$\text{and} \qquad \frac{r_2}{r_1} = 1 + \frac{d}{r_0 \pm \beta x},$$

where r_0 is the inner radius of the channel at the inlet of the channel ($x = 0$), β is the modulus of curvature of the spiral, and x is the distance measured from the inlet along the inner wall with the positive sign corresponding to outward flow and the negative sign corresponding to inward flow. The mean friction factor over any distance L measured from the inlet is then simply

$$f_m = \frac{1}{L}\int_0^L f\,dx. \tag{17}$$

Specific calculated results are not presented here for true spirals because of the several additional parameters (β, r_0, and L) and the absence of experimental data for confirmation.

Concluding Remarks

The finite-element modeling described herein provides the first detailed velocity fields for angular flow in the annulus between two concentric cylinders (equivalent to a torus of rectangular cross section) for large and infinite aspect ratios. The hypothetical pressure gradient for such flows was simulated by an equivalent body force.

For an infinite aspect ratio and an inner-radius-to-gap ratio of 20.17 the motion was found to be wholly angular for values of

$$Dn = \frac{du_{\theta m}\rho}{\mu}\left(\frac{d}{r_1}\right)^{1/2}$$

below a critical value of 37.31. For greater values of Dn a secondary motion in the form of pairs of counterrotating vortices was computed. The wavelength of these pairs of vortices was determined by trial and error as that distance that resulted in the minimal mean rate of flow for a given pressure gradient. The relationship between the wavelength of the vortices and the Dean number as so determined is in good agreement with the prior analysis of Finlay et al. (1988) for a large finite aspect ratio as well as with the visualizations of Kelleher et al. (1980) and of the present work.

The computed value of the critical Dean number is in good agreement with prior results obtained by stability analyses as well as with the results of the current visualizations.

The computed friction factor expressed in terms of $f_{ave}Re_d$ as a function of Dn for $Dn_c \leq Dn \leq Dn_{cu}$ is well represented by Eq. 15, which can be generalized for other conditions in the form of Eq. 16.

The approximate calculations of Walowit et al. (1964) using the Galerkin method indicate that the critical value of the Dean number and the corresponding wavelength obtained herein for an inner-radius-to-gap ratio of 20 differ only about 1% from those for the classical case of an infinite ratio.

The computations for finite aspect ratios of 5, 12 and 16 reveal a boundary layer type of secondary motion below a critical value of the Dean number, while for larger values a number of counterrotating vortices similar to those for an infinite aspect ratio were computed plus one very extended vortex near each end wall.

The computed patterns of flow for finite aspect ratios are in excellent agreement with the visualizations of Cheng et al. (1977).

The computed friction factors for finite aspect ratios are consistent with one another, with those for an infinite aspect ratio, and with the asymptotic solution for no curvature, but cover an insufficient range of Dn to support the construction of a generalized correlating equation.

Although all of the present and prior results are actually for toroidal flow, they are presumed to be applicable, as described herein, as a reasonable approximation for spiral coils.

Finally, the computed velocity fields, which are necessarily only illustrated herein, have been found to be sufficient in

scope, detail, and accuracy to support the derivation of corresponding values for the heat-transfer coefficients on the inner and outer walls.

Acknowledgments

The support of the National Science Foundation for the experimental work through SBIR grants ISI 8560638 and ISI 8619609 and for the computations through grant MSM 900037P at the Pittsburgh Supercomputing Center is gratefully acknowledged.

Notation

b = height of regime of finite-element computations
f = Fanning friction factor = $[2(\tau_w)_{ave}]/\rho u_m^2$
f_{ave} = Fanning friction factor based on average radius
G = arbitrary body force, m^2/s^2
h = axial length of annulus
n = index of summation
P = dynamic pressure due to velocity
r = radial coordinate
$r_{ave} = (r_1 + r_2)/2$
Re_d = Reynolds number based on $d = du_m \rho/\mu$
u_r = velocity in the r direction
u_z = velocity in the z direction
u_θ = velocity in the θ direction

Greek letters

θ = angular coordinate
μ = dynamic viscosity
ρ = specific density
τ_{w1} = shear stress on the inner wall of an annulus
τ_{w2} = shear stress on the outer wall of an annulus
$\psi\{h/d\}$ = function defined by Eq. 8

Subscripts

a = value for purely angular flow
c = critical value for onset of vortical motion
cu = critical value for onset of undulating vortical motion
m = mean value

Literature Cited

Baurmeister, U., and H. Brauer, "Laminare Strömung und Wärmeübergang in Rohrwendeln und Rohrspiralen," *Ver. Deut. Eng. Forschungsh.*, 593 (1979).

Brewster, D. B., P. Grosberg, and A. H. Nissan, "The Stability of Viscous Flow between Horizontal Concentric Cylinders," *Proc. Roy. Soc. (London), Ser. A*, **251**, 76 (1959).

Cheng, K. C., and M. Akiyama, "Laminar Forced Convection Heat Transfer in Curved Rectangular Channels," *Int. J. Heat Mass Transfer*, **13**, 471 (1970).

Cheng, K. C., R.-C. Lin, and J.-W. Ou, "Fully Developed Channel Flow in Curved Rectangular Channels," *J. Fluids Eng., Trans. ASME*, **98**, 41 (1976).

Cheng, K. C., J. Nakayama, and M. Akiyama, "Effect of Finite and Infinite Aspect Ratios on Flow Patterns in Curved Rectangular Channels," *Proc. Int. Symp. Flow Visualization*, Tokyo, Japan, p. 109 (1977).

Chowdhury, K., H. Linkmeyer, M. K. Bassiouny, and H. Martin, "Analytical Studies on the Temperature Distribution in Spiral Plate Heat Exchangers: Straightforward Design Formulae for Efficiency and Mean Temperature Difference," *Chem. Eng. Process.*, **19**, 183 (1985).

Churchill, S. W., and R. Usagi, "A General Expression for the Correlation of Rates of Transfer and Other Phenomena," *AIChE J.*, **18**, 1121 (1972).

Cliffe, K. A., and T. Mullin, "A Numerical and Experimental Study of Anomalous Modes in the Taylor Experiment," *J. Fluid Mech.*, **153**, 243 (1985).

Dean, W. R., "Fluid Motion in Curved Channels," *Proc. R. Soc. London, Ser. A*, **121**, 402 (1928).

Finlay, W. H., J. B. Keller, and J. H. Ferziger, "Instability and Transition in Curved Channel Flow," *J. Fluid Mech.*, **194**, 417 (1988).

Goldstein, S., ed., *Modern Developments in Fluid Dynamics*, Vol. 1, Oxford Univ. Press (Clarendon), Oxford, p. 315 (1938).

Jones, A. R., S. A. Lloyd, and F. J. Weinberg, "Combustion in Heat Exchangers," *Proc. R. Soc. (London), Ser. A*, **360**, 97 (1978).

Kelleher, M. D., D. L. Flentie, and R. J. McKee, "An Experimental Study of the Secondary Flow in a Curved Rectangular Channel," *J. Fluids Eng., Trans. ASME*, **102**, 92 (1980).

Ligrani, P. M., and R. D. Niver, "Visualization of Dean Vortices in a Curved Channel with 40 to 1 Aspect Ratio," *Phys. Fluids*, **31**, 3605 (1988).

Ligrani, P. M., W. H. Finlay, W. A. Fields, S. J. Fugua, and C. S. Subramanian, "Features of Wavy Vortices in a Curved Channel from Experimental and Numerical Studies," *Phys. Fluids A*, **4**, 695 (1992).

Reid, W. H., "On the Stability of Viscous Flow in a Curved Channel," *Proc. R. Soc. (London), Ser. A*, **244**, 186 (1958).

Retallick, W. B., S. W. Churchill, and M. R. Strenger, "Catalytic Air Cleaner," U.S. Patent No. 4,911,894 (Mar. 27, 1990).

Targett, M. J., S. W. Churchill, and W. B. Retallick, "The Incineration of Contaminants in Air with a Double-Spiral Heat Exchanger/Catalytic Reactor," *Proc. 4th World Congress of Chemical Engineering*, Karlsruhe, Germany, p. 842 (1991).

Targett, M. J., W. B. Retallick, and S. W. Churchill, "Solutions in Closed Form for a Double-Spiral Heat Exchanger," *Ind. Eng. Chem. Res.*, **31**, 658 (1992).

Taylor, G. I., "Stability of Viscous Liquid Contained between Two Rotating Cylinders," *Phil. Trans. R. Soc. (London), Ser. A*, **223**, 289 (1923).

de Saint-Venant, B., "Mémoire sur la Torsion des Prismes, avec des Considérations sur leur Flexion, ainsi que sur l'Équilibre Intérieur des Solides Élastiques en Genéral, et des Formules Practiques pour le Calcul de leur Résistance à Divers Efforts s'Exercant Simultanément," *Mémoires des Savants Étrangers*, Vol. 14, **233**, Paris (1855).

Walowit, J., S. Tsao, and R. C. Di Prima, "Stability of Flow Between Arbitrarily Spaced Concentric Cylindrical Surfaces Including the Effect of a Radial Temperature Gradient," *J. Appl. Mech.*, **31**, 585 (1964).

Winters, K. H., and R. C. G. Brindley, "Multiple Solutions for Laminar Flow in Helically-Coiled Tubes," Harwell Report AERE-R-11373 (Aug., 1984).

Winters, K. H., "A Bifurcation Study of Laminar Flow in a Curved Tube of Rectangular Cross-Section," *J. Fluid Mech.*, **180**, 343 (1987).

Manuscript received Mar. 14, 1994, and revision received June 16, 1994.